

Consider next the determinations of the quenching rate constant carried out at constant ionic strength (0.75 or 2.00 M). In these experiments sodium sulfate was added to maintain the ionic strength. This introduces a second ion-pairing term (K_2) and also a rate constant k_0'' for the deactivation of the sulfate ion pair. The resulting description can be simplified by assuming the two ion-pairing constants are identical ($K = K_1 \cong K_2$),²¹ yielding the equation

$$k_{\text{obsd}} = \frac{k_0 + k_0''KC + (k_{\text{ox}} + k_0' - k_0'')K[\text{C}_2\text{O}_4^{2-}]}{1 + KC} \quad (12)$$

where C is the sum $[\text{C}_2\text{O}_4^{2-}] + [\text{SO}_4^{2-}]$. According to this equation the constant a of eq 10 is equal to $(k_0 + k_0''KC)/(1 + KC)$, and $k_q = \{K(k_{\text{ox}} + k_0' - k_0'')\}/(1 + KC)$. The difference in the values of k_q for the two series can be shown to be due to the dependence of the ion-pairing constant on ionic strength. The Fuoss equation gives $K = 6.7 \text{ M}^{-1}$ ($\mu = 0.75 \text{ M}$) and $K = 4.3 \text{ M}^{-1}$ ($\mu = 2.00 \text{ M}$). The theoretical ratio of the slope at $\mu = 2.00 \text{ M}$ to that at 0.75 M is then 0.44. The experimental ratio is $(1.57 \times 10^5)/(3.59 \times 10^5) = 0.43$. This agreement validates the reaction scheme and the data treatment.

The values of k_{ox} , the unimolecular rate constant for quenching within the ion pair, are listed in Table I. They were calculated from the values of k_q and K under the assumption that $k_0' \cong k_0''$. In that case $k_{\text{ox}} = k_q(1 + KC)/K$. A radius of 6.8 Å was used in the calculations for all the complexes examined.

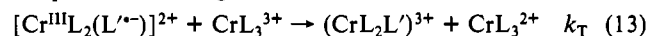
The Transient Intermediate. The quenching of $\text{Cr}(\text{phen})_3^{3+}$, $\text{Cr}(5\text{-Cl-phen})_3^{3+}$, and $\text{Cr}(5\text{-Mephen})_3^{3+}$ by oxalate yields an intermediate, T. In these cases the $\text{CO}_2^{\cdot-}$, formed in reactions 3 and 4, apparently does not transfer an electron directly to CrL_3^{3+} to produce CrL_3^{2+} and CO_2 , as it does for $\text{Cr}(\text{bpy})_3^{3+}$ and $\text{Cr}(4,4'\text{-Me}_2\text{bpy})_3^{3+}$. T has a broad absorption in the visible region, as shown by the spectrum obtained by quenching of $^*\text{Cr}(5\text{-Cl-phen})_3^{3+}$ by oxalate ions, Figure 4.

Two possibilities seem likely for the identity of T. Electron transfer from $\text{CO}_2^{\cdot-}$ to the phenanthroline ring may produce a ligand radical species, $\text{T} = [\text{Cr}^{\text{III}}\text{L}_2(\text{L}^{\cdot-})]^{2+}$, analogous to the known²³ $\text{Li}^+\text{bpy}^{\cdot-}$. Alternatively, $\text{CO}_2^{\cdot-}$ may add to the ligand,

producing a substituted-ring radical, $\text{T} = [\text{Cr}^{\text{III}}\text{L}_2(\text{L}'^{\cdot-})]^{2+}$. In either case the visible spectrum will have the features of a phen $^{\cdot-}$ species. Examples of both types of reactivity of coordinated polypyridines exist. A ligand radical species was proposed in the reaction of $\text{Ru}(\text{bpy})_3^{3+}$ with e_{aq}^- ,²⁴ and a ligand addition species, in the reaction of $^*\text{CH}_2\text{OH}$ with $\text{Cr}(\text{phen})_3^{3+}$.²⁵ The assignment is a difficult one to make for the latter reaction, since the spectral data given²⁵ for the intermediate do not rule out the ligand radical species.^{26,27}

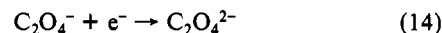
It is interesting to note that $\text{Cr}(\text{bpy})_3^{3+}$ reacts with $^*\text{CH}_2\text{OH}$ to give $\text{Cr}(\text{bpy})_3^{2+}$ directly.²⁵ Thus, the difference between the bipyridine and phenanthroline complexes observed in our work with $\text{CO}_2^{\cdot-}$ parallels that found with $^*\text{CH}_2\text{OH}$. The radical produced by the oxidation of $\text{H}_2\text{edta}^{2-}$, on the other hand, yields long-lived intermediates with both types of complexes. Ultimately, however, we arrive at no convincing rationale as to the different species formed with bpy and phen complexes.

T reacts with ground-state CrL_3^{3+} to produce what appears to be CrL_3^{2+} by its electronic spectrum. The following seems to be the process occurring:

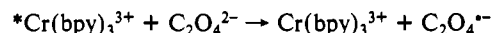


The rate constants for reaction 13 vary somewhat with the nature of the quencher, implying that different quenchers ($\text{H}_2\text{edta}^{2-}$ or oxalate) produce different intermediates T. This would be consistent with ligand addition. The differences in the rate constants are, however, not large enough to permit unambiguous distinction between the two possibilities.

Finally, we should consider the thermodynamics of the quenching process. The calculated one-electron reduction potential for $\text{C}_2\text{O}_4^{2-}$ is



$E^\circ = 0.60 \text{ V}$.²⁸ The initial step of the quenching process



is therefore a favorable one, with $\Delta E = 0.86 \text{ V}$.

Acknowledgment. This work was supported by the U.S. Department of Energy, Office of Basic Energy Sciences, Chemical Sciences Division, under Contract W-7405-Eng-82. We are grateful to Professor C. J. Frieden for a copy of the program KINSIM.

- (21) This is a reasonable proposition, since SO_4^{2-} and $\text{C}_2\text{O}_4^{2-}$ have very similar radii: Pringle, G. E.; Broadbent, T. A. *Acta Crystallogr.* **1965**, *19*, 426.
 (22) This approximation is a reasonable one. Indeed the value of k_0'' ($3.3 \times 10^4 \text{ s}^{-1}$, from the intercept of k_{obsd} vs $[\text{C}_2\text{O}_4^{2-}]$ in the absence of SO_4^{2-}) is close to that of k_0 ($1.4 \times 10^4 \text{ s}^{-1}$) for the tris(bipyridine) complex. It is, however, not possible to evaluate k_0' , and so further direct comparisons cannot be made.
 (23) McWhinnie, W. R.; Miller, J. D. *Adv. Inorg. Chem. Radiochem.* **1969**, *12*, 135.

- (24) Jonah, C. D.; Matheson, M. S.; Meisel, D. *J. Am. Chem. Soc.* **1978**, *100*, 1449.
 (25) Venturi, M.; Emmi, S.; Fuochi, P. G.; Mulazzani, Q. G. *J. Phys. Chem.* **1980**, *84*, 2160.
 (26) Konig, E.; Kremer, S. *Chem. Phys. Lett.* **1970**, *5*, 87.
 (27) Calculated from the two-electron potential ($\text{H}_2\text{C}_2\text{O}_4/\text{CO}_2$) and the $\text{CO}_2/\text{CO}_2^{\cdot-}$ potential (-1.9 V) and the K_{a1} and K_{a2} values for $\text{H}_2\text{C}_2\text{O}_4$.

Contribution from the Department of Chemistry and Biochemistry, University of California, Los Angeles, California 90024, and Department of Chemistry, University of California, Santa Barbara, California 93106

Photochemical Cleavage of Carbonate in $\text{Cp}^*\text{Rh}(\text{CO}_3)\cdot 2\text{H}_2\text{O}$

Maher Henary,[†] William C. Kaska,^{*†} and Jeffrey I. Zink^{*†}

Received December 19, 1988

Irradiation of $\text{Cp}^*\text{Rh}(\text{CO}_3)\cdot 2\text{H}_2\text{O}$ in THF at 351 nm leads to photochemical cleavage of the carbonate ligand to form carbon dioxide and a metal-oxo intermediate that reacts with the starting material to produce the dimeric $[(\text{Cp}^*\text{Rh})_2(\text{OH})_3]^+$ complex. The photoreaction is wavelength dependent. The reaction quantum yield in THF is 0.24 ± 0.03 with 351-nm irradiation and is immeasurably small at wavelengths longer than 488 nm. The characterization of the photoproducts and the photochemical mechanism are discussed.

The photochemical reactivity of metal-carbonate complexes has not been well studied. Most earlier work shows that ready

elimination of CO_2 occurs with the concomitant formation of highly reactive species.¹⁻³ The carbonate ligand is photochem-

[†]University of California, Los Angeles.

^{*}University of California, Santa Barbara.

(1) Palmer, D. A.; van Eldik, R. *Chem. Rev.* **1983**, *83*, 651.

(2) Krishnamurthy, K. V.; Harris, G. M.; Sastri, V. S. *Chem. Rev.* **1970**, *70*, 171.

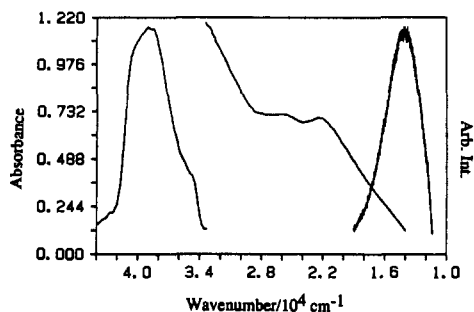


Figure 1. Electronic absorption spectrum (left) and emission spectrum (right) of $\text{Cp}^*\text{Rh}(\text{CO}_3)\cdot 2\text{H}_2\text{O}$. The absorption spectrum in the high-energy regions was obtained from a 1.17×10^{-3} M room-temperature THF solution and that in the low-energy region from a 2.22×10^{-3} M solution. The emission spectrum was obtained from a powder at 10 K.

ically interesting because it offers an easy method of binding the elements of carbon dioxide to a metal. (The carbonate ion is in thermodynamic equilibrium with carbon dioxide and water.) It thus offers a potential route to the photochemically driven splitting of carbon dioxide.

The half-sandwich compounds of rhodium and iridium with the pentamethylcyclopentadiene ligand that were first studied by King⁴ and Maitlis^{5,6} have generated novel chemistry in the form of C–H metalation⁷ and the existence of stable high-valent compounds. Electron-releasing effects of the five methyl groups on the cyclopentadienyl ring strengthen the metal–ring bond by increasing the electron density on the metal atom. This effect should stabilize moderate oxidation states, especially with metals that can coordinate hard ligands like carbonate or an oxygen atom in the form of a metallo–oxo complex.

In order to explore the photochemical reaction pathways of the carbonate ligand, we are investigating the photochemistry of organometallic carbonate complexes. In this paper, we describe work directed toward an understanding of carbonate photolysis with (pentamethylcyclopentadienyl)rhodium complexes.

Experimental Section

The compounds were synthesized by literature methods.⁵ The IR spectrum of the starting material $\text{Cp}^*\text{Rh}(\text{CO}_3)\cdot 2\text{H}_2\text{O}$ in the solid state contains bands at 1604 and 1313 cm^{-1} characteristic of the bidentate carbonate ligand.^{5,8} The IR spectrum of the dimer $[\{\text{Cp}^*\text{Rh}\}_2(\text{OH})_3]^+$ complex in the solid state contained a strong band at 3250 cm^{-1} due to $\nu(\text{OH})$ and a band at 470 cm^{-1} due to $\nu(\text{Rh}-\text{OH})$.⁵

Electronic absorption spectra were obtained by using a Cary 14 and an HP 8451 diode-array spectrophotometer. All spectra were obtained in anhydrous THF or absolute ethanol in matched quartz cells at room temperature. Infrared spectra were obtained in KBr disks or in THF solution on a Mattson Cygnus 25 FTIR spectrophotometer. Gas chromatography experiments were carried out by using a HP 5890A gas chromatograph with a medium-polarity DB-17 column and temperature programming. The emission spectrum was obtained by using the instrument previously described.⁹

Results and Discussion

Electronic Spectroscopy. The electronic absorption spectrum of the monocarbonate complex in THF contains two weak bands at 375 nm ($\epsilon = 329 \text{ M}^{-1} \text{ cm}^{-1}$) and 450 nm ($\epsilon = 317 \text{ M}^{-1} \text{ cm}^{-1}$) and a more intense band ($\epsilon = 1011 \text{ M}^{-1} \text{ cm}^{-1}$) at 250 nm as shown in Figure 1. The electronic absorption spectrum of dimeric $[\{\text{Cp}^*\text{Rh}\}_2(\text{OH})_3]\text{Cl}$ contains two bands, a weak band at 357 nm

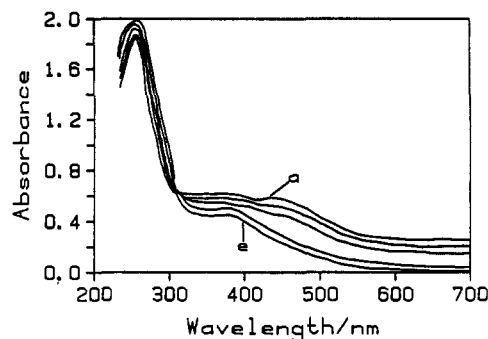


Figure 2. Absorption spectroscopic changes during 351-nm irradiation of a 1.83×10^{-3} M solution of $\text{Cp}^*\text{Rh}(\text{CO}_3)\cdot 2\text{H}_2\text{O}$ in THF at room temperature. The irradiation times are (a) 0, (b) 10, (c) 20, (d) 30, and (e) 45 min. The spectrum of $[\{\text{Cp}^*\text{Rh}\}_2(\text{OH})_3]^+$ is identical with spectrum e.

($\epsilon = 250 \text{ M}^{-1} \text{ cm}^{-1}$) and an intense band at 250 nm.

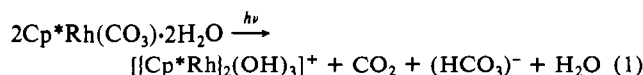
The intense peak that appears at 250 nm in both $\text{Cp}^*\text{Rh}(\text{CO}_3)\cdot 2\text{H}_2\text{O}$ and $[\{\text{Cp}^*\text{Rh}\}_2(\text{OH})_3]\text{Cl}$ is assigned to the Cp^* to rhodium LMCT transition. LMCT bands in this wavelength region are well-known in a large number of rhodium(III) complexes.¹⁰ The appearance of this band in the spectra of both the hydroxo dimer and the carbonate complex rules out charge transfer from the carbonate ligand.

The two low-energy peaks in the electronic absorption spectrum of $\text{Cp}^*\text{Rh}(\text{CO}_3)\cdot 2\text{H}_2\text{O}$ at 375 and 450 nm shown in Figure 1 are assigned to d–d transitions. Their wavelengths and molar extinction coefficients are typical of spin-allowed ligand field transitions in rhodium(III) complexes.¹⁰ The lowest energy peak at 357 nm ($\epsilon = 250 \text{ M}^{-1} \text{ cm}^{-1}$) in the spectrum of $[\{\text{Cp}^*\text{Rh}\}_2(\text{OH})_3]\text{Cl}$ is also assigned to a ligand field transition. It occurs at higher energy than the lowest ligand field band in $\text{Cp}^*\text{Rh}(\text{CO}_3)\cdot 2\text{H}_2\text{O}$ because the hydroxyl ligands provide a stronger ligand field splitting than the carbonate ligand.

$\text{Cp}^*\text{Rh}(\text{CO}_3)\cdot 2\text{H}_2\text{O}$ is luminescent at low temperature when excited at wavelengths of 488 nm and below. The emission spectrum, shown in Figure 1, is independent of the wavelength of excitation. The bandwidth and band energy are similar to those of many other rhodium(III) complexes.¹⁰ Because the lowest energy excited state of the $\text{Cp}^*\text{Rh}(\text{CO}_3)\cdot 2\text{H}_2\text{O}$ complex is d–d in nature, the emission band in Figure 1 is correspondingly assigned to the lowest energy ligand field excited state.

Photochemistry. The photochemical reactivity of $\text{Cp}^*\text{Rh}(\text{CO}_3)\cdot 2\text{H}_2\text{O}$ was studied by irradiating a 1.83×10^{-3} M solution in anhydrous THF or absolute ethanol in a stirred quartz cell with an argon ion laser. The photon flux was 2.65×10^{16} photons/s (15 mw) at 351 nm or 2.74×10^{16} photons/s at 364 nm as measured with a calibrated power meter.

The overall photochemical reaction from irradiation of $\text{Cp}^*\text{Rh}(\text{CO}_3)\cdot 2\text{H}_2\text{O}$ is given in eq 1. The metal-containing photoproduct of the reaction is the hydroxo-bridged dimeric complex. The carbonate ligand is cleaved resulting in carbon dioxide production.



The spectral changes resulting from the photochemical reaction of eq 1 are shown in Figure 2. Spectrum a is that of the starting carbonate complex and spectrum e is that of the metal-containing photoproduct. An isosbestic point is observed at 310 nm. The absorption spectrum of an authentic sample of the hydroxo-bridged dimer is identical with that of the photoproduct.

It is interesting to note that the stoichiometry of the metal complexes in eq 1 requires 2 mol of starting material to form 1

- (3) Blake, D. M.; Mersecchi, R. *J. Chem. Soc., Chem. Commun.* **1971**, 1405.
- (4) King, R. B. *Coord. Chem. Rev.* **1976**, *20*, 155.
- (5) Nutton, A.; Bailey, P. M.; Maitlis, P. M. *J. Chem. Soc., Dalton Trans.* **1981**, 1997. Kang, J. W.; Maitlis, P. M. *J. Organomet. Chem.* **1971**, *30*, 127.
- (6) Maitlis, P. M. *Coord. Chem. Rev.* **1982**, *43*, 385.
- (7) Janowicz, A. H.; Bergman, R. G. *J. Am. Chem. Soc.* **1982**, *104*, 352. Hoyano, J. K.; Graham, W. A. G. *J. Am. Chem. Soc.* **1982**, *104*, 3723. Jones, W. D.; Feher, F. J. *J. Am. Chem. Soc.* **1982**, *104*, 4240.
- (8) Bertin, E. P.; Penland, R. B.; Mizushima, S.; Guagliano, J. V. *J. Am. Chem. Soc.* **1959**, *81*, 3818. Fujita, J.; Martell, A. E.; Nakamoto, K. *J. Phys. Chem.* **1962**, *36*, 339.
- (9) Tutt, L.; Zink, J. I. *J. Am. Chem. Soc.* **1986**, *108*, 5830.

- (10) Thomas, T. R.; Crosby, G. A. *J. Mol. Spectrosc.* **1971**, *38*, 118. Peterson, J. D.; Watts, R. J.; Ford, P. C. *J. Am. Chem. Soc.* **1976**, *98*, 3188. Demas, J. N.; Crosby, G. A. *J. Am. Chem. Soc.* **1970**, *92*, 7262. Osborn, R. D.; Wilkinson, G. *J. Chem. Soc.* **1964**, 3168.

mol of the dimeric product. The photochemical reaction is thus the unusual case where the fixed 2:1 ratio of reactants to products leads to the observed isosbestic point in contrast to the more common case where the isosbestic point is required by a 1:1 ratio.^{11,12}

The photoproducts of reaction were also characterized by IR spectroscopy. The spectrum of the starting material $\text{Cp}^*\text{Rh}(\text{CO}_3)\cdot 2\text{H}_2\text{O}$ in the solid state contains bands at 1604 and 1313 cm^{-1} characteristic of the bridging bidentate carbonate ligand.^{5,8} In a THF solution these bands are obscured by the solvent bands. The IR spectra of $\text{Cp}^*\text{Rh}(\text{CO}_3)\cdot 2\text{H}_2\text{O}$ in both the solid state and in a 1.83×10^{-3} M THF solution do not contain any bands in the region between 2200 and 2400 cm^{-1} . However, as the photolysis proceeded, a sharp band appeared at 2340 cm^{-1} and grew in intensity. This band is characteristic of the presence of CO_2 in solution.¹³ A solution of THF saturated with CO_2 contains a strong band at this position. These results show that photolysis cleaves the carbonate ligand, releasing carbon dioxide.

A potential precursor of the observed carbon dioxide photoproduct could be uncomplexed carbonate ion if the intact ion were photodissociated from the starting metal complex. Under acidic conditions the equilibrium between the carbonate ion and carbon dioxide and water is shifted toward the latter two molecules. In order to rule out this possibility, the photochemical reactivity was studied by irradiating a 5×10^{-5} M solution of the carbonate complex at 351 nm in THF containing a 2:1 mole ratio excess of triethylamine. The photoproducts were characterized by IR spectroscopy. The IR spectrum after photolysis contains the band at 2340 cm^{-1} characteristic of carbon dioxide.¹³ This band does not appear in the spectrum of the solution before photolysis. These results under basic conditions show that the origin of the carbon dioxide is not free carbonate ion and support the interpretation that the origin of the carbon dioxide is photochemical cleavage of the coordinated carbonate ligand.

The photoproduction of carbon dioxide was corroborated by GC studies during photolysis. The gas chromatograms of the starting material in THF before, during, and after photolysis were compared with those from pure THF and CO_2 -saturated THF. The irradiated solutions contained the peak characteristic of CO_2 .

Reaction Quantum Yields. A plot of the change of concentration of $\text{Cp}^*\text{Rh}(\text{CO}_3)\cdot 2\text{H}_2\text{O}$ versus time at 375 nm was linear and passed through the origin for irradiation times up to 45 min. The quantum yield for dissociation of CO_2 and formation of the hydroxy-bridged dimer is 0.24 ± 0.03 .

The photochemical reactivity was also studied in absolute ethanol in order to determine if the solvent played an important role in the photochemical reactivity. A 1.83×10^{-3} M solution of $\text{Cp}^*\text{Rh}(\text{CO}_3)\cdot 2\text{H}_2\text{O}$ was irradiated at 351 nm with an argon ion laser under conditions identical with those described above. The quantum yield for CO_2 loss and formation of the hydroxy-bridged dimer was 0.25 ± 0.03 , identical within the experimental uncertainty with that in THF.

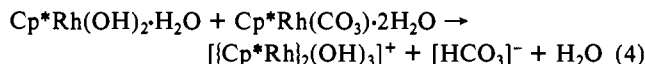
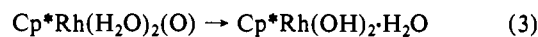
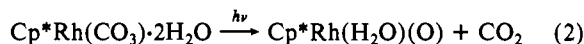
The photochemical reaction was strongly wavelength dependent. Photochemical reactivity in THF was studied at longer wavelengths by using the 488- and 514.5-nm lines from an argon ion laser. Laser fluxes of 3.68×10^{16} photons/s and 3.88×10^{16} photons/s, respectively, were used. These wavelengths are well within the ligand field absorption bands of the starting material (Figure 1) but are well removed from the tail of the 250-nm charge-transfer band. No changes in the absorption spectra were observed for irradiation times up to 1 h. The IR spectra of the reaction mixtures did not contain a peak in the region between 2200 and 2400 cm^{-1} , which indicated that there is no dissociation of CO_2 on photolyzing $\text{Cp}^*\text{Rh}(\text{CO}_3)\cdot 2\text{H}_2\text{O}$ in THF at these wavelengths.

The photochemical reactivity of $\text{Cp}^*\text{Rh}(\text{CO}_3)\cdot 2\text{H}_2\text{O}$ arises from the high-energy charge-transfer excited state and not from the

lower energy ligand excited states. The 351-nm excitation line falls in a region of the absorption spectrum containing both the low-energy tail of the 350-nm LMCT band and the high-energy side of the 375-nm d-d band. It is difficult to determine exactly how far to low energy the tail of the CT band extends, but from the shape of the band in Figure 1, it is likely that the absorbance from this band is negligible at wavelengths longer than about 400 nm. The absence of measurable photochemical activity at an irradiation wavelength of 488 nm which is well within the lowest energy d-d band shows that the d-d state is photochemically inactive and that the reactivity originates from the higher energy charge-transfer state.

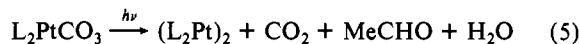
Photofragmentation of the Carbonate. The photofragmentation of the carbonate ligand follows the most favorable thermodynamic path by cleaving a carbon-oxygen bond and forming carbon dioxide. The most interesting feature of this reaction is the formation of a reactive oxo species (vide infra). A second possible photochemical fragmentation pathway (although of higher energy) that could have occurred is the cleavage of two carbon-oxygen bonds to form carbon monoxide and the peroxo complex. The energy needed to drive this reaction would have to be provided by the photon.

The reaction sequence leading to the formation of the dimer is not known exactly but most likely involves an oxo primary photoproduct that is trapped by coordinated water molecules to give the hydroxy dimer as shown in eq 2-4. The primary pho-

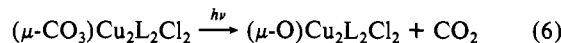


tochemical step is photogeneration of a reactive coordinated oxo ligand that reacts internally with the aquo ligands to form the dihydroxo species. Subsequent thermal reactions with an unphotolyzed molecule of the starting material lead to the loss of the elements of the bicarbonate ion (or alternatively a molecule of carbon dioxide and the hydroxide ion) and formation of the stable trihydroxo-bridged dimer.

The reactive oxo group that is produced as a result of carbonate photolysis can be chemically useful¹⁴⁻¹⁸ when the oxo group is not internally deactivated on the complex. For example, photolysis of (carbonato)bis(triphenylphosphine)platinum(II) in methanol results in the production of 1 mol of CO_2 and the dimer $(\text{L}_2\text{Pt})_2$ (eq 5).³ In addition, methanol is oxidized to form acetaldehyde.³



Another recently reported photoreaction of a metal carbonate complex illustrates that stabilization of the oxo group on the metal can lead to the reversible sequence of carbon dioxide photolysis and coordination. Photolysis of $(\mu\text{-CO}_3)\text{Cu}_2\text{L}_2\text{Cl}_2$ ($\text{L} = 1,10$ -phenanthroline) causes efficient carbon dioxide loss¹⁹ (eq 6). In



this case, the oxo ligand was stabilized by bridging two copper atoms, and further reactions involving the oxo group did not occur.

Acknowledgment. This work was supported by the Office of Naval Research. We thank K.-S. Shin for assistance with the figures.

(11) Mayer, R. G.; Drago, R. S. *Inorg. Chem.* **1976**, *15*, 2010.

(12) Liu, P.-H.; Zink, J. I. *Inorg. Chem.* **1977**, *16*, 3165.

(13) Ozin, G. A.; Huber, H.; McIntosh, D. *Inorg. Chem.* **1978**, *17*, 1472.

(14) Symposium on Chemistry of Transition Metal Alkoxide, Oxo, and Related Compounds, 196th National Meeting, of the American Chemical Society, Los Angeles, CA, 1988; papers INOR 157-164.

(15) Rappe, A. K.; Goddard, W. A. *J. Am. Chem. Soc.* **1982**, *104*, 3287.

(16) Holm, R. H. *Chem. Rev.* **1987**, *87*, 1401.

(17) Griffith, W. P. *Coord. Chem. Rev.* **1970**, *5*, 459.

(18) Dickson, M. K.; Dixit, N. S.; Roundhill, D. M. *Inorg. Chem.* **1983**, *22*, 3130.

(19) Henary, M.; Zink, J. I. *J. Am. Chem. Soc.* **1988**, *110*, 5582.